Available online at www.sciencedirect.com
SCIENCE DIRECT®
Global and Planetary Change 49 (2005) 28–46
GLOBAL AND PLANETARY CHANGE
www.elsevier.com/locate/gloplacha

Palaeoceanography of the Banda Sea, and Late Pleistocene initiation of the Northwest Monsoon

Michelle I. Spooner[a,*], Timothy T. Barrows[b], Patrick De Deckker[a], Martine Paterne[c]

[a]*Department of Earth and Marine Sciences, The Australian National University, Canberra ACT 0200, Australia*
[b]*Department of Nuclear Physics, Research School of Physical Sciences and Engineering, The Australian National University, Canberra ACT 0200, Australia*
[c]*Laboratoire des Sciences du Climat et de l' Environment, Unité Mixte CNRS/CEA, Domaine du CNRS, Avenue de la Terrasse, Gif-sur-Yvette 91198, France*

Received 24 June 2003; received in revised form 5 May 2005; accepted 19 May 2005

Abstract

This paper details the Late Quaternary palaeoceanography of the Banda Sea based on analysis of core SHI 9016, located east of Timor. This core is located below the pathway of the Indonesian Throughflow, at a depth of 1805 m bsl. Planktonic foraminifera assemblages, the $\delta^{18}O$ and $\delta^{13}C$ of the foraminifer *Globigerinoides ruber*, and the total carbonate content of each sample were used to reconstruct the vertical structure of the water column through the past ~80,000 yr.

Today, the core site is characterised by high sea-surface temperature and high precipitation, which results in the formation of a low-salinity boundary layer. Sea-surface temperature estimates down core indicate minimal cooling during the last glacial maximum. Mean sea-surface temperatures ranged between 29.8 °C and 26.6 °C for the past ~80,000 yr; sea-surface seasonality never increased above 3 °C. In addition, the abundance of the planktonic foraminifera *Neogloboquadrina dutertrei*, *Neogloboquadrina pachyderma*, and *Globigerinoides quadrilobatus* indicates that the mixed layer (the low-salinity boundary layer of the Throughflow) thinned during Marine Isotope Stages 3 and 2. This enhanced a deep chlorophyll maximum (DCM) layer. The Northwest Monsoon was less intense for about 60,000 yr and then 'switched on' at ~15,000 cal yr BP. This thickened the mixed layer, reducing the DCM, and increased SST seasonality in the Banda Sea.

Keywords: Banda Sea; Indonesian Throughflow; Indo-Pacific; Late Quaternary; monsoon; deep chlorophyll maximum; planktonic foraminifera

1. Introduction

The flow of surface water from the Pacific Ocean into the Indian Ocean through the Indonesian Archipelago, called the Indonesian Throughflow, represents an important oceanographic link between

* Corresponding author. Tel.: +61 2 6125 2064; fax: +61 2 6125 5544.
E-mail address: michelle@ems.anu.edu.au (M.I. Spooner).

0921-8181/$ - see front matter © 2005 Elsevier B.V. All rights reserved.
doi:10.1016/j.gloplacha.2005.05.002

these two major oceans. This region is one of three global centres of tropical convection where warm, low-salinity water is injected into the global circulation system (Kinkade et al., 1997). The heat and freshwater carried by the Throughflow into the Indian Ocean participates in global oceanographic circulation (Gordon, 1986). However, locally, the Throughflow strengthens the Indian Ocean South Equatorial Current, the Leeuwin Current, and affects the heat budget of the Indian Ocean (Godfrey, 1996).

Hydrological characteristics are modified within the Throughflow by the regional climate. The 'Indo-Pacific Warm Pool' (WP) is the largest single expanse of warm water on the planet with a sea-surface temperature (SST) consistently higher than 28 °C (Yan et al., 1992). The high temperature of the WP enhances the transfer of moisture from the sea surface to the atmosphere. As a result, this region has the most extensive coverage of organised deep convective cloud on Earth. Within the 26.5–29 °C range of SST, organised convection is much increased (Waliser and Graham, 1993; De Deckker et al., 2003). Because of high precipitation, there is a net gain of freshwater over evaporation, resulting in warm, low-salinity surface water within the Throughflow. This low-salinity cap is frequently referred to as the "barrier layer" (sensu Lukas and Lindstrom, 1991).

Despite the importance of the Indonesian region, little is known about how the oceanography responded to climate change in the past. During the last glacial maximum (LGM), a reduction in sea level may have significantly modified circulation by significantly changing the land margins of the Indonesian Archipelago. During most of the glacial/interglacial cycle, the Java and Flores Seas (Sunda Shelf), the Strait of Malacca, and a large portion of the Banda and Arafura Seas were exposed above water (De Deckker et al., 2003). The region between 20°N–20°S and 90°E–130°E presently has 4.1 times more water than land. It is believed that during the LGM, the same area covered by water was only 1.6 times the area compared to land (De Deckker et al., 2003). Such large changes are likely to have impacted upon the monsoonal regime across the Indonesian Archipelago, which would influence the paleoceanography of the Banda Sea.

Palaeoclimatic studies undertaken within the Indonesian region have produced a range of results, some of which are contradictory. This paper aims to improve understanding of the palaeoceanography of the Indonesian Archipelago since Marine Isotope Stage (MIS) 5a. The location of core SHI 9016 (8°27.35′S, 128°14.28′E) in the Banda Sea, the largest and deepest of the basins within the Indonesian Archipelago, is well placed to record oceanographic conditions in the past. Using planktonic foraminifera, we investigate changes in SST and potential disruptions to the upper surface layer of the Banda Sea because of changes in the Asian Monsoon.

2. Regional setting

2.1. Climate

The modern climate of the Indonesian Archipelago is dominated by biannual monsoonal circulation. Heavy rain accompanies northwesterly winds between November and March (Austral summer), during the Northwest (NW) Monsoon. The dry season corresponds to the Southeast (SE) Monsoon period from May to September (Austral winter). The resultant climate in northern Australia, southern New Guinea, the Lesser Sunda Islands, and Timor is characterised by a strong seasonal contrast in rainfall (van der Kaars et al., 2000).

The intertropical convergence zone (ITCZ) is the driving force behind monsoonal variability. The ITCZ, a pressure trough where the southeast and northeast trade winds meet, usually lies about 10°–15° north of the equator in the Austral winter and migrates south, close to or over northern Australia in summer (Hobbs, 1998). At present, the yearly movement of the ITCZ in Australasia is larger than anywhere else in the world (Singh and Agrawal, 1976).

The interactions between the high-pressure system over Australia and a low-pressure system over Asia during winter (August) promote southwesterly winds over the Indian subcontinent. Conversely, a low-pressure system over Australia and a high-pressure system over Asia during summer (February) promote northeasterly winds over Southeast Asia (Tomczak and Godfrey, 1994).

During the Austral summer, the NW Monsoon gathers large amounts of moisture while crossing the sea from the Asian high-pressure belt on its way to the ITCZ, which has shifted south. The northwesterly winds are then moisture-laden and a low-pressure gradient is established between the Pacific and Indian Oceans (Ahmad et al., 1995). At the ITCZ, the moisture-laden air rises, resulting in heavy rains (van der Kaars et al., 2000). During the Austral winter, the SE Monsoon originates from the Southern Hemisphere high-pressure belt and is relatively dry and cool (van der Kaars et al., 2000). The semi-permanent South Pacific high-pressure system, which generates the southeast trade wind flow, is centred between 85°–100°W and 27°–37°S (Hobbs, 1998).

2.2. Oceanography

A horizontal pressure gradient causes the flow of Pacific Ocean surface water into the Indian Ocean. The volume of water transported from the Pacific to the Indian Ocean ranges between 2 and 24 Sv (1 Sverdrup = 10^6 m^{-3} s^{-1}) (Godfrey, 1996). The Throughflow also provides the only connection between the main thermocline of two major oceans at low latitudes (Hautala et al., 1996). The Throughflow can be subdivided into: (1) the shallow western region (<75 m) over the Sunda Shelf, primarily the Java and South China Seas, and (2) the eastern region, consisting of a series of deep (>1000 m) basins connected by shallower sills (Hautala et al., 1996).

Pacific intermediate waters enter the Indonesian Archipelago and follow a western or eastern route (Fig. 1). The eastern route is the pattern of flow which presently influences conditions above core site SHI 9016. The eastern route, through the Halmahera and Molucca Seas, reaches the Banda Sea from the north. From the Banda Sea, there are two deep passages to the Indian Ocean: (1) the Ombai Strait, between the Alor and Timor Islands; and (2) the Timor Passage, between the Roti Islands and the Australian continental shelf (Molcard et al., 1996).

The WP region is recognized for its high rainfall, and as a site of formation of low-density oceanic water. Excess precipitation/runoff over evaporation in the western Indonesian Archipelago, and subsequent vertical mixing down into the water column, can be seen in surface water (0–200 m) that is fresher (S<34.50) than either of the Pacific sources in the western Banda Sea and in the outflow passages (Timor and Ombai Straits) (Hautala et al., 1996; Fig. 2).

Presently, the water masses of the Banda Sea and adjacent areas are highly influenced by the biannual monsoonal system, creating 'seasonal' cycles in the area. Observations of SST at the site of core SHI 9016 show a difference between the two 'seasons.' During the NW Monsoon, SST is 29 °C, and is 26.8 °C during the SE Monsoon (Levitus and Boyer, 1994). During a shorter period of observation, Troelstra et al. (1989) found that SST varies between 30.1 °C (Sulawesi) and 28.3 °C (Timor) during non-upwelling periods. Kinkade et al. (1997) found that during the SE Monsoon, SST is 1 °C lower in the western seas (from 29.2 °C to 28.1 °C) and 2.5 °C lower (from 29.0 °C to 26.6 °C) in the eastern seas. This is due to increased vertical mixing during the SE Monsoon (Kinkade et al., 1997; see Fig. 3).

Within the Throughflow, the thermocline appears to adjust to changes in thickness of the low-salinity surface layer and to the biannual monsoon regime (Wijffels et al., 1996). Bray et al. (1996) estimated a thermoclime depth of ~110–120 m at the 21 °C isotherm east of Timor. Measurements by van Iperen et al. (1993) suggest that the thermocline adjusts seasonally, clearly showing uplift of the thermocline during the SE Monsoon: from 70 to 90 m in February/March to 30–40 m in August. Therefore, the thermocline can be observed to be the shallowest during the period of maximum Throughflow transport (Fig. 3). During the SE Monsoon (May–September), currents flow to the west from the Arafura/Banda area, creating 'upwelling' of cooler, more nutrient-rich waters in the eastern Banda Sea (Wyrtki, 1961; Troelstra and Kroon, 1989). This can be observed by an almost linear increase in chlorophyll *a* with decreasing SST in August (Kinkade et al., 1997).

Wyrtki (1961) indicated that during the NW Monsoon (November–March), strong eastward currents from the Java and Flores Seas flow into the Banda Sea. Winds are not favourable for removal of the water from the Banda Sea into the Indian Ocean.

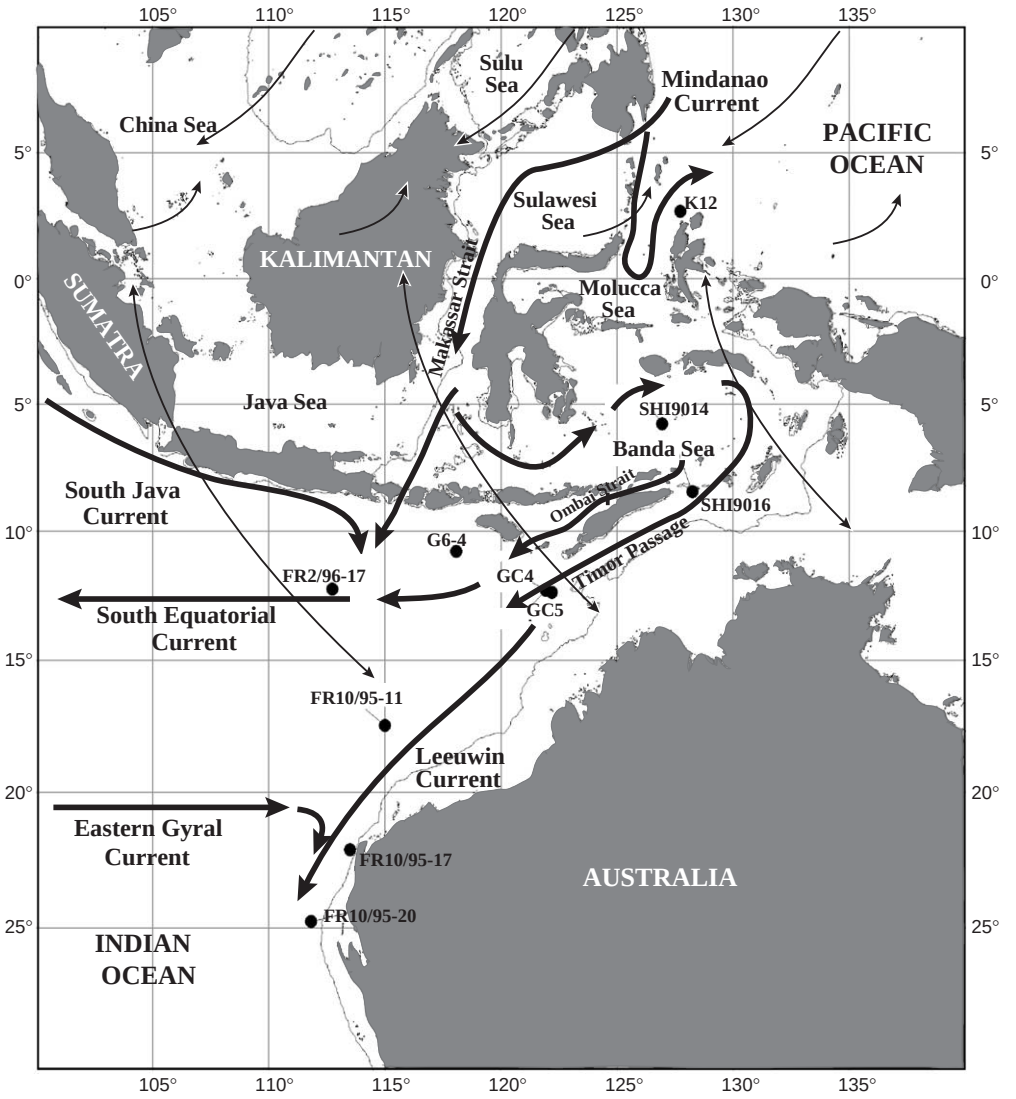

Fig. 1. The location of deep-sea cores within the Australasian region referred to in the text and the principal water movements associated with the Indonesian Throughflow. Core K12 was analysed by Barmawidjaja et al. (1993), and SHI 9014 by Ahmad et al. (1995) and van der Kaars et al. (2000). Core SHI 9016 was analysed in this paper and was also investigated by Gingele et al. (2001). Cores GC 4 and GC 5 were analysed by Müller and Opdyke (2000), and core G6-4 by Wang et al. (1999). Cores FR 2/96-17, FR10/95-20, and FR10/95-17 were analysed by Martinez et al. (1999) and Takahashi and Okada (2000), and core FR10/95-11 by Martinez et al. (1999). Currents from Wijffels et al. (1996).

Consequently, low-salinity water accumulates in the Banda Sea and depresses the thermocline (Fig. 3). The pressure gradient from the Pacific to the Indian Ocean is also weak; therefore the Throughflow from the Pacific to the Indian Ocean is reduced during the NW Monsoon (Wyrtki, 1987). The 'downwelling' season is characterised by oligotrophic conditions (Troelstra and Kroon, 1989).

3. Planktonic foraminifera and the deep chlorophyll maximum

There have been very few studies of foraminifera conducted within the Indonesian Archipelago. Information supplied by the Snellius-II Expedition, cruise G5, in 1984 still remains the main body of work for this region. Most studies have concentrated on present

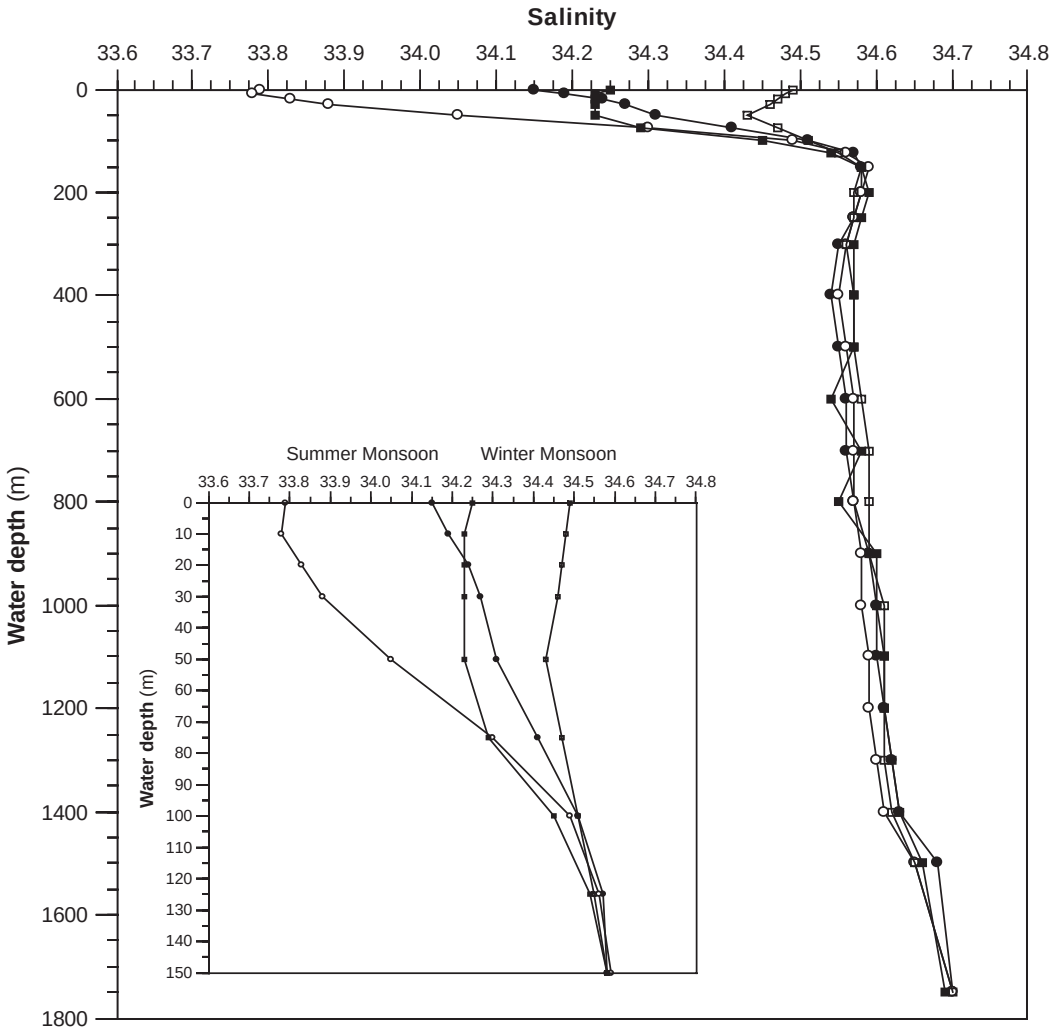

Fig. 2. Salinity measurements for the entire water column above core SHI 9016 for the four seasons (Levitus et al., 1994). Note the dramatic changes in salinity near the surface caused by differences in local precipitation in the region: high precipitation corresponds to the Northwest Monsoon and high salinity to the Southeast Monsoon. Insert shows the salinity change in the upper 150 m of the water column. Closed circles = summer temperature profile; open circles = autumn temperature profile; closed squares = winter temperature profile; open squares = spring temperature profile.

ecological patterns (e.g., Troelstra and Kroon, 1989) and Gieskes et al. (1988) showed that these seasonal differences are reflected in the phytoplankton stock. During the fertile upwelling period (SE Monsoon), phytoplankton biomass is two times higher than during the downwelling season (NW Monsoon) (Troelstra and Kroon, 1989). Planktonic foraminifera abundances respond to these changes in phytoplankton abundance.

Plankton tows from the Snellius-II Expedition, cruise G5, found a total of 28 planktonic foraminiferal species in the Banda Sea. The species *Globigerinoides ruber*, *Globigerinoides quadrilobatus*, *Globigerinita glutinata*, *Neogloboquadrina dutertrei*, and *Globorotalia menardii* are the most abundant, with less frequent *Globigerinella aequilateralis* and *Pulleniatina obliquiloculata*. In addition, *Globigerina bulloides* is common (5–23% of the fauna), associated with a shallower thermocline during the SE Monsoon (Troelstra and Kroon, 1989). The abundance of *N. dutertrei* and *G. bulloides* in planktonic tows of the Snellius-II

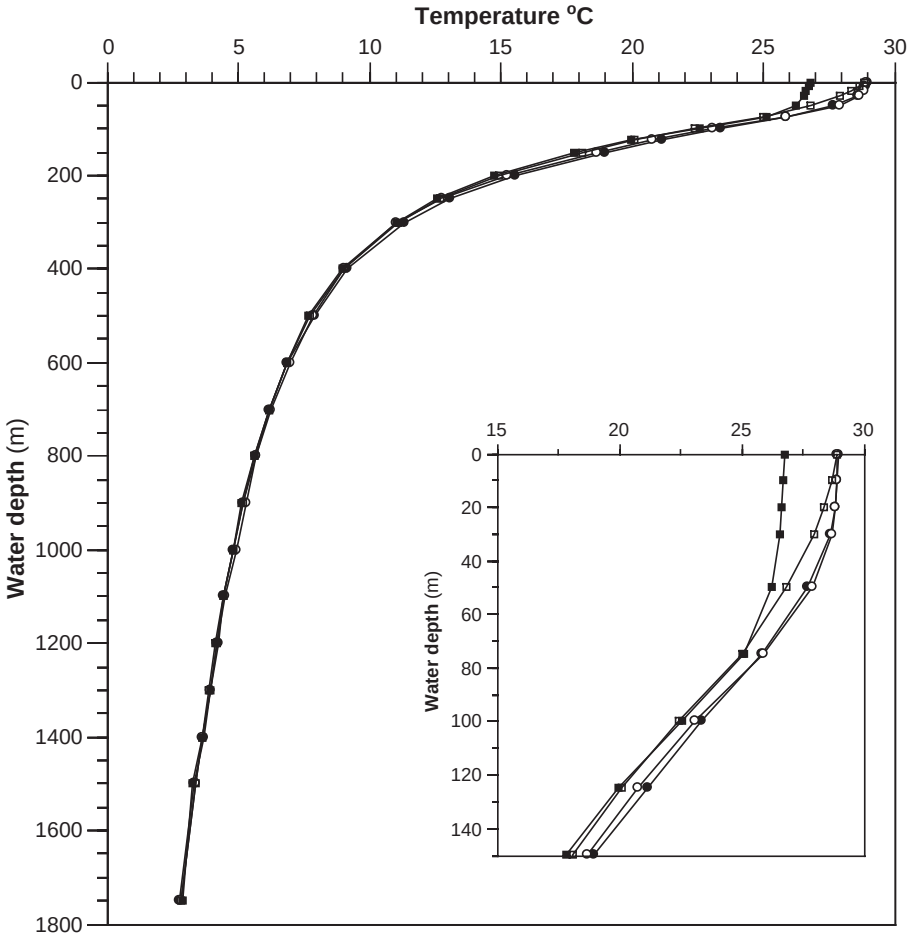

Fig. 3. The water column temperature profiles of the four seasons above the core site SHI 9016 (Levitus et al., 1994). Note the thermocline is fixed below ~100 m for all of the seasons. Insert shows the temperature profiles in the upper 150 m. Note the SST change in winter resulting from Southeast Monsoon winds cooling and mixing the upper ~50 m of the water column. The symbols are the same as Fig. 2.

Expedition suggests that a deep chlorophyll maximum (DCM) layer develops during the SE Monsoon.

A DCM develops when the thermocline lies above or near the light compensation depth and causes an increase in chlorophyll production at the bottom of the photic zone (Fairbanks and Wiebe, 1980; Barmawidjaja et al., 1993). The DCM layer may be seasonal or a permanent feature, which is fuelled with new nutrients by cross-isopycnal or along isopycnal mixing (Hayward, 1987).

Herbivorous foraminifera with specific temperature tolerances, such as *N. dutertrei* and *Neogloboquadrina pachyderma*, exploit the DCM and this results in an increase of relative abundance of these species. *G. bulloides* is also regarded as typical of upwelling systems and shows a preference for productive cold waters (Bé and Hutson, 1977; Hemleben et al., 1989). However, Hilbrecht (1996) recognised that *N. dutertrei* increased when *G. bulloides* decreased due to different availabilities of phytoplankton and competition.

Studies within the Indonesian Throughflow and the eastern Indian Ocean, such as Barmawidjaja et al. (1993) and Martinez et al. (1999), have used planktonic foraminifera to indicate possible reductions in temperature of the eutrophic layer and the increase of nutrients in the photic zone promoting DCM characteristics. The core top study of Martinez et al. (1999) showed the abundance of species such

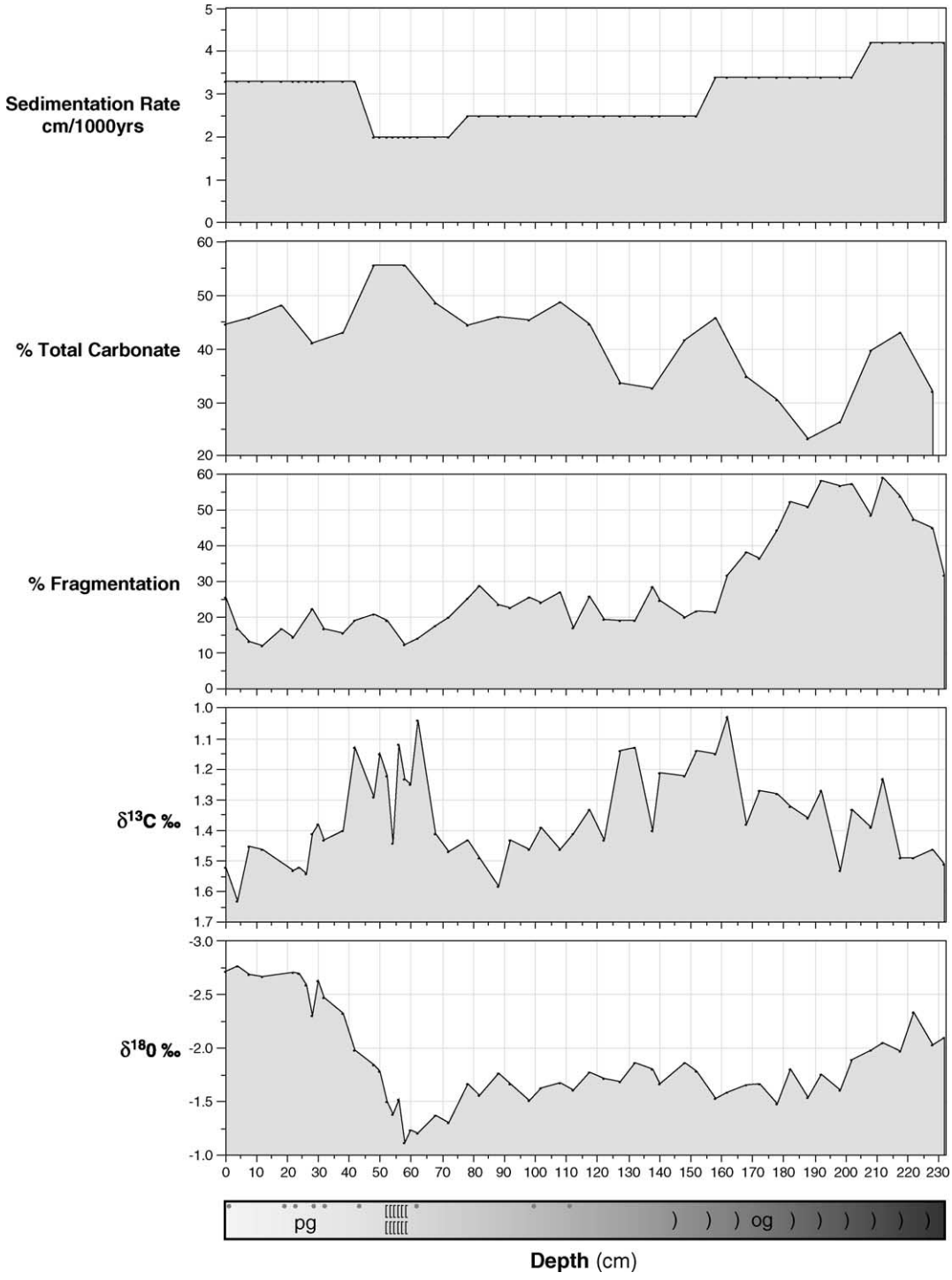
Sedimentation Rate
cm/1000yrs
% Total Carbonate
% Fragmentation
δ13C ‰
δ18O ‰
pg
og
Depth (cm)

as *N. pachyderma*, *N. dutertrei*, and *G. bulloides* varied around the region and depended on the mixed-layer thickness and the intensity of the Java upwelling system.

4. Materials and methods

4.1. Core details

In 1990, a collaborative French and Indonesian cruise, named 'SHIVA,' took a selection of cores among the Indonesian islands. Core SHI 9016 was taken at 8°27.35′S, 128°14.28′E, at the depth of 1805 m bsl (Fig. 1).

The sediments within core SHI 9016, particularly on the basis of grain size, indicate continuous pelagic sedimentation (Fig. 4). Sediments alter down core from pale grey, foraminiferal-rich clay (0–50 cm) to dark grey foraminiferal-rich clay (60–146 cm). Between 50 and 60 cm, faint laminations are visible, indicating lack of bioturbation. At 148 cm, there is another colour change to olive grey clay, with some foraminiferal sand lenses that possibly indicate winnowing effects.

The foraminiferal sand lenses are less conspicuous slightly below 180 cm (see Fig. 4). Below 232 cm, there is a sharp wavy contact and a corresponding grain size and colour change. We infer that the clay fraction has been removed between 232 cm and 360 cm by winnowing processes. This is supported by the carbonate content, which is over 90%. Winnowing of smaller foraminifera species such as *Globoturborotalita rubescens* may have also occurred. Reworking occurs from 232 cm to the end of the core (650 cm). Therefore, only the upper 232 cm of SHI 9016 is described here. Fragmentation is high below 160 cm, reducing the reliability of the results in the interval 160–232 cm. The data from this paper are stored at the *WDC-A for Palaeoclimatology* (http://www.ngdc.noaa.gov/paleo) and the *Australian Quaternary Data Archive* (http://www.aqua.org.au/archive.html).

Table 1
Radiocarbon dates from core SHI 9016

Laboratory code number	Depth (cm)	^{14}C dates	^{14}C cal yr (BP)
GifA 101566	0–1	2200 ± 60	1710 ± 100
GifA 101567	18–19	5450 ± 70	5740 ± 130
GifA 101568	22–23	6000 ± 110	6330 ± 130
GifA 101569	28–29	7520 ± 110	7920 ± 130
GifA 101570	32–33	7810 ± 110	8180 ± 150
GifA 101571	42–43	11210 ± 140	12720 ± 190
GifA 101572	58–59	16800 ± 180	19360 ± 360

4.2. Isotope analysis

Each sample, consisting of ~3 g of sediment from 4 or 6 cm intervals, was wet-sieved. Approximately 15 *G. ruber* were handpicked from the 150–250 mm size fraction for isotope analysis. The foraminifera were cleaned in 100% ethanol to remove any clay. The stable isotopes in these samples were analysed in a Finnigan Mat 251 Mass Spectrometer at the Research School of Earth Sciences at the Australian National University. The analytical error for δ^{18}O is better than ± 0.08‰ and for δ^{13}C is better than ± 0.05‰ (Joe Cali, personal communication).

4.3. Age model

Ten samples, consisting of 10 mg of *G. ruber*, were radiocarbon-dated by AMS. Target preparations followed standard techniques at the Tandetron of Gif-sur-Yvette (Tisnérat-Laborde et al., 2001). The radiocarbon dates were used to construct an age model for the upper sections of SHI 9016 (Table 1). Dates were calibrated using the INTCAL98 marine curve and the Calib 4.3 program (Stuiver et al., 1998). For the oceanic reservoir correction, the regional ΔR mean for NW Australia and Java of 64 ± 24 was used (Bowman, 1985; Southon et al., 2002).

To obtain an age model for the older part of the core, the δ^{18}O data were correlated against the SPECMAP age model of Martinson et al. (1987). Events used and their corresponding ages are listed in Table 2. Likely errors for this age model range from ± 1370

Fig. 4. Stable isotope data, fragmentation, and carbonate percentage versus depth in core SHI 9016. The schematised core log of SHI 9016 shows a gradational colour change from pale grey (pg) clay to olive grey (og) clay with depth. Dots on the log indicate location of AMS radiocarbon samples. Laminations are also highlighted on the schematic log at 50–60 cm as shown by square brackets and foraminifera sand lenses from 140 cm as shown by curved brackets.

Table 2
Age model for core SHI 9016 and corresponding $\delta^{13}C$ and $\delta^{18}O$ results for depth and age

Depth (cm)	Dating	Age model	$\delta^{18}O$	$\delta^{13}C$	$\%CaCO_3$
0	^{14}C	1711	−2.72	1.52	44.65
4		2605	−2.77	1.63	–
8		3499	−2.69	1.45	45.69
12		4394	−2.67	1.46	–
18	^{14}C	5735	–	–	48.18
22	^{14}C	6328	−2.71	1.53	–
24		6859	−2.70	1.52	–
26		7389	−2.59	1.54	–
28	^{14}C	7920	−2.31	1.41	41.01
30		8051	−2.63	1.38	–
32	^{14}C	8181	−2.48	1.43	–
38		10904	−2.33	1.40	43.09
42	^{14}C	12719	−1.99	1.13	–
48		15211	−1.85	1.29	55.55
50		16041	−1.79	1.15	–
52		16872	−1.50	1.22	–
54		17702	−1.39	1.44	–
56		18533	−1.52	1.12	–
58	^{14}C	19363	−1.12	1.23	55.55
60		19969	−1.24	1.25	–
62		20574	−1.21	1.04	–
68		22392	−1.38	1.41	48.49
72		23603	−1.31	1.47	–
78	MIS 3.1	25420	−1.67	1.43	44.34
82		27289	−1.56	1.49	–
88		30093	−1.77	1.58	46.07
92		31962	−1.67	1.43	–
98		34766	−1.51	1.46	45.38
102		36636	−1.63	1.39	–
108		39440	−1.68	1.46	48.80
112		41309	−1.61	1.41	–
117.5	3.13	43880	−1.78	1.33	44.55
122		45844	−1.72	1.43	–
127.5		48246	−1.69	1.14	33.67
132	3.3	50210	−1.87	1.13	–
137.5		52011	−1.81	1.40	32.74
140		52830	−1.67	1.21	–
148	3.31	55450	−1.87	1.22	41.65
152	4.0	58960	−1.79	1.14	–
158		60884	−1.53	1.15	45.69
162		62166	−1.59	1.03	–
168	4.22	64090	−1.66	1.38	34.81
172		65245	−1.67	1.27	–
178		66978	−1.49	1.28	30.56
182		68134	−1.81	1.32	–
188		69866	−1.54	1.36	23.31
192		71022	−1.76	1.27	–
198		72755	−1.61	1.53	26.46
202	5.0	73910	−1.90	1.33	–
208		75512	−1.99	1.39	39.69
212		76580	−2.05	1.23	–
217.5		78182	−1.98	1.49	43.05
222	5.1	79250	−2.34	1.49	–
228		80318	−2.03	1.46	32.11
232		81030	−2.10	1.51	–

Ages calibrated using ^{14}C values indicated up to 19343 ^{14}C cal yr BP. Martinson et al. (1987) isotopic stack is used after the age limitation of radiocarbon dating. Isotopic events are indicated. MIS = Marine Isotope Stage.

cal yr BP at stage 2.2 to ±5560 cal yr BP at stage 4.0 (Martinson et al., 1987).

4.4. Planktonic foraminifera

Counts of planktonic foraminifera were made on splits of the >150 μm fraction to exclude juvenile specimens. At least 400 planktonic foraminifera per sample were identified to species level. The number of fragments was also recorded to give an indication of the preservation status of the sample. We follow the taxonomy of Saito et al. (1981). However, we use the earlier synonym of *G. quadrilobatus* for *Globigerinoides sacculifer* to incorporate all its morphological forms (Chapronière, 1991).

4.5. Total carbonate

To determine total carbonate content, samples were taken throughout the core at 10-cm intervals. Each sample was homogenised into a fine powder in a mortar to aid in the dissolution of the sample. Titrations were conducted by using Metrohm Ion analysis, 716 DMS Titrino Series 6.0, and AG CH-9101 pH meter; the precision of these instruments is ±0.04 %. Approximately 0.3 g of sediment was dissolved in 1 M HCl and titrated against 0.5 M NaOH.

4.6. Modern analogue technique

Sea-surface temperatures were estimated from the planktonic foraminifera assemblage data using the modern analogue technique (MAT), in conjunction with the AUSMAT-F4 database (Barrows and Juggins, 2005). This database represents an upgrade of the AUSMAT-F3 database (Martinez et al., 2002). We estimated mean annual SST (T_{mean}), and the temperature of the warmest and coolest months. In a tropical

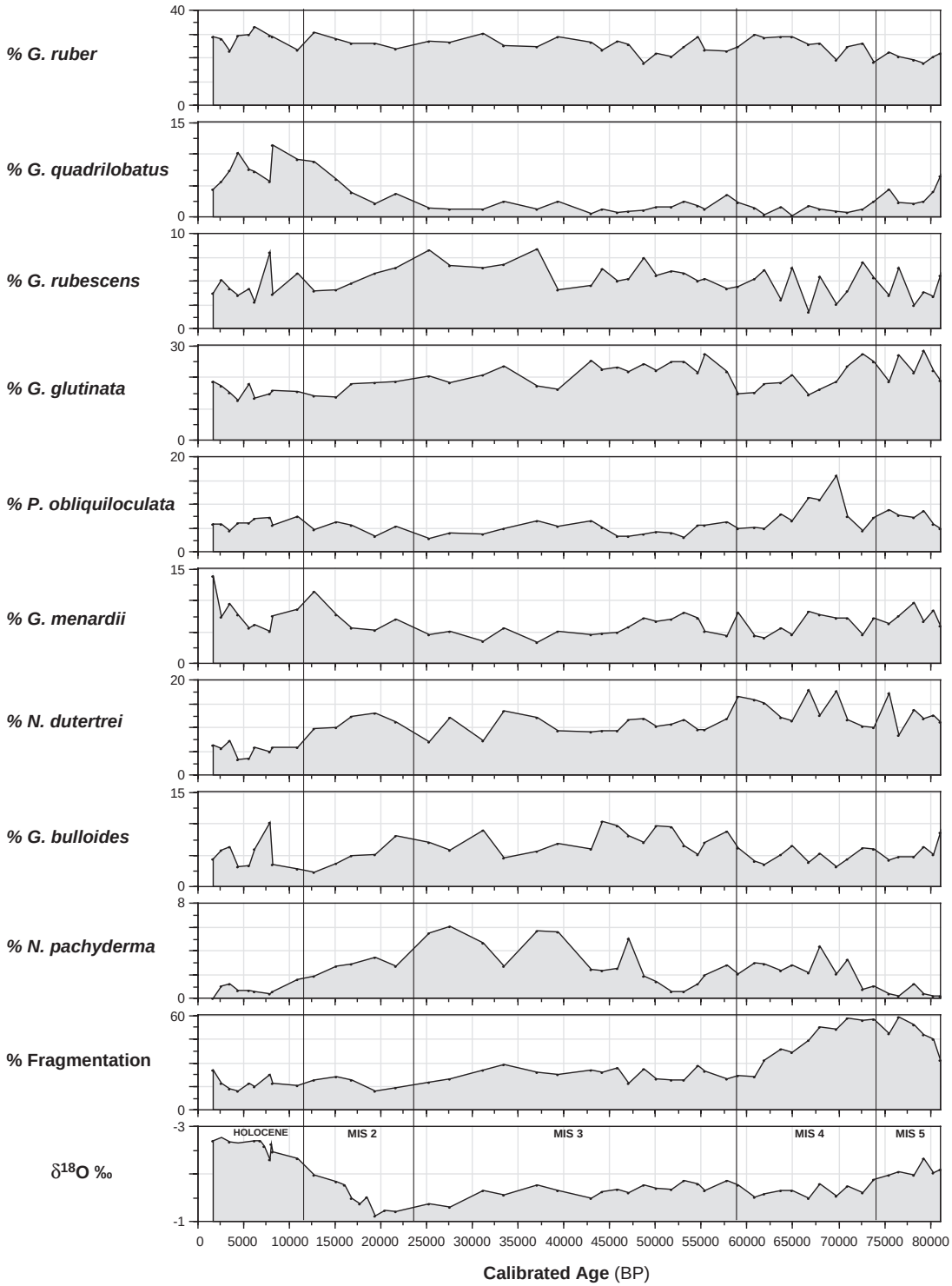

Fig. 5. Relative abundances of the most common foraminifera (>5%) in SHI 9016, and fragmentation percentage. MIS=Marine Isotope Stage.

monsoonal setting, the months with the most extreme temperatures are usually not the calendar months in the middle of summer and winter. The temperature minimum (T_{min}) of the sea surface corresponds to conditions during the SE Monsoon, when upwelling that cools the surface occurs (Troelstra and Kroon, 1989; van Iperen et al., 1993) and there is increased vertical mixing (Gordon, 1986; Kinkade et al., 1997). The sea-surface temperature maximum (T_{max}) reflects the NW Monsoon due to apparent downwelling during this period (December; according to Levitus and Boyer, 1994) (Wyrtki, 1961; Troelstra and Kroon, 1989; Fig. 6). This highlights the importance of reconstructing the temperature of these months whenever they occur throughout the year (Barrows and Juggins, 2005).

In addition to SST parameters, we estimated temperature at 50 m, 100 m, and 150 m depth (using data for the core top analogs from Levitus and Boyer, 1994). These depth levels are important because the highest concentration of foraminifera lives below the surface, in the mixed layer, and at the top of the thermocline. The 100 m and 150 m depth levels are at the base of the photic zone where a DCM could develop in regions with a thin mixed layer such as the Banda Sea. Therefore, these temperature variables should be more representative of the changes influencing the assemblage.

Each SST estimate was calculated as the mean of the best 10 analogues from the global database, using the squared chord distance as the dissimilarity coefficient. The distance to the nearest analogue, the mean distance, and the standard deviation were also calculated to assess the quality of the analogue.

5. Results

5.1. Stable isotope record

Results from the stable isotope analyses are given in Table 2. Event 2.2 during the LGM occurs at 58 cm and is directly dated at 19,360 ^{14}C cal yr BP. This is close to 18,200 ± 1500 cal yr BP determined by Barrows and Juggins (2005) for this event in the western Pacific Ocean. The difference between the LGM and core top δ^{18}O is 1.6‰, which is 0.5–0.6‰ greater than the ice volume effect (Schrag et al., 1996).

The maximum range of δ^{13}C is from 1.04‰ at 21,700 cal yr BP to 1.63‰ during the Holocene. Therefore, the maximum variation of δ^{13}C is 0.59‰ over the past ~80,000 cal yr BP (Fig. 4). The carbonate is relatively enriched in ^{12}C during the stadials MIS 2 and 4 (Fig. 5). Conversely, the carbonate is relatively enriched in ^{13}C during the interstadials at the end of MIS 5a, during MIS 3, and the Holocene.

5.2. Planktonic foraminifera abundance

Fragmentation and foraminiferal abundances in SHI 9016 are plotted in Fig. 5. Fragmentation is generally low but is highest in the oldest part of the core before 60,000 yr BP (Fig. 5). The solution-resistant species *P. obliquiloculata* is significantly more abundant during this period. However, the solution-susceptible species (like *G. glutinata*) are not noticeably less abundant during this period compared to other parts of the core. Sand lenses occur in the lower part of the core, indicating winnowing through bottom current activity. Therefore, fragmentation might be the result of mechanical abrasion. Increased etching of foraminifera fragments also points to more corrosive water at the sea floor during this period.

5.2.1. Thermocline dwellers

Thermocline-dwelling foraminifera were most abundant between 15,000 and 80,000 cal yr BP. The relative abundance of *N. dutertrei* is lowest during the Holocene. *N. pachyderma* is most abundant during MIS 3 and is only a minor species during the Holocene interval.

G. bulloides is most abundant during stadial periods, apart from a brief increase early in the Holocene (see Fig. 5). Several minor deep-dwelling species only appear during the LGM and/or MIS 3. These include *Globorotalia crassaformis*, *Globorotalia truncatulinoides*, *Hastigerina parapelagica*, and sinistral *N. pachyderma.* These were grouped with other thermocline-dwelling species in Fig. 6.

Fig. 6. Temperature variations in core SHI 9016: temperature mean (T_{mean}; °C), temperature mean standard deviation (S.D.; °C), temperature maximum (T_{max}; °C), temperature maximum standard deviation (°C), temperature minimum ($T_{min;}$ °C), temperature minimum standard deviation (°C), relative abundance of mixed-layer dwelling species, and relative abundance of thermocline dwelling species.

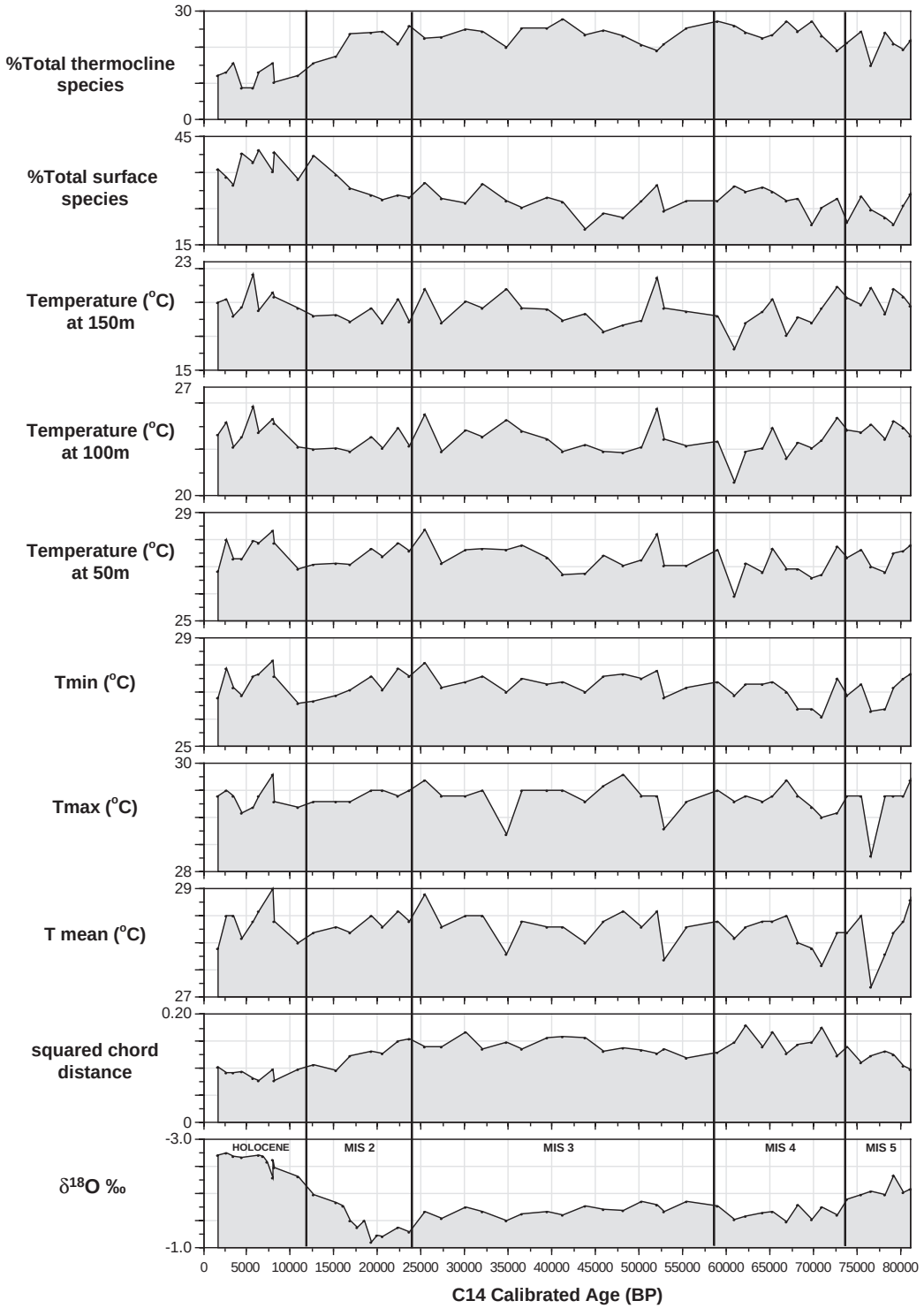
%Total thermocline species
30
0
%Total surface species
45
15
Temperature (°C) at 150m
23
15
Temperature (°C) at 100m
27
20
Temperature (°C) at 50m
29
25
Tmin (°C)
29
25
Tmax (°C)
30
28
T mean (°C)
29
27
squared chord distance
0.20
0
δ18O ‰
-3.0
-1.0
HOLOCENE
MIS 2
MIS 3
MIS 4
MIS 5
0 5000 10000 15000 20000 25000 30000 35000 40000 45000 50000 55000 60000 65000 70000 75000 80000
C14 Calibrated Age (BP)

5.2.2. Mixed-layer dwellers

Mixed-layer dwellers are most abundant during the Holocene interval (Figs. 5 and 6). *G. ruber* is the most common species throughout SHI 9016, representing at least ~20% of the population. Apart from minor decreases in abundance during the warmer intervals of MIS 5a and early in MIS 3, *G. ruber* abundance is constant through the core (Fig. 5).

Together with *G. ruber*, the abundance of *G. quadrilobatus* indicates the presence and temperature of the mixed layer. This is a shallow, mixed-layer species mainly residing in the upper 0–75 m of the ocean (Hemleben et al., 1989). This species rapidly increases after the LGM into the Holocene (Fig. 5). The highest relative abundance of this species was 11.5% at 8200 ^{14}C cal yr BP and was least abundant during MIS 3 and 2. As a euryhaline species that prefers oligotrophic conditions and temperatures >24 °C, this reduction may be due to cooling of the mixed layer.

Pink *G. ruber* appears in SHI 9016 at 55,400 cal yr BP. This is long after the local extinction date of 125,000 cal yr BP in the Pacific and Indian Oceans (Thompson et al., 1979). This may indicate bottom current reworking during MIS 4 and 5. This appears to be confirmed by a change of carbonate percentages and foraminifer fragmentation (see Section 5.3).

5.3. $CaCO_3$ content of core SHI 9016

Total carbonate content is highest during the LGM, at a value of 56% (Fig. 4), with high percentages throughout MIS 2 and 3. Notable drops in carbonate percentage occur during MIS 5a and early in MIS 3. The earlier interval corresponds to a period of intense fragmentation where carbonate preservation was at its lowest level (Fig. 4).

Sedimentation rates are greatest in the Holocene and MIS 4 at rates of 3.3 cm 1000 yr^{-1} and 3.4 cm 1000 yr^{-1}, respectively (Fig. 4). Sedimentation rates are slowest during MIS 2 and 3 at 2.0 cm 1000 yr^{-1} and 2.5 cm 1000 yr^{-1}, respectively. The average sedimentation rate for the core (0–232 cm) is 2.9 cm 1000 yr^{-1}. A reduction in terrestrial sediment input during MIS 2 and 3 would explain the higher carbonate percentages (Fig. 5).

5.4. Sea-surface temperature reconstruction

Sea-surface temperature estimates from the MAT are shown in Fig. 6. All of the SST estimates have squared chord distances of <0.2, indicating that the samples have good analogues in the AUSMAT-F3 database. The highest-quality estimates are in the youngest interval (<16 ka), where the distances are ~0.1 or less. Below this level, distances are mostly >0.1.

Modern observations of SST for the core site are 29.7 °C and 26.6 °C for T_{max} and T_{min}, respectively (Levitus and Boyer, 1994). The MAT SST estimates for T_{max} and T_{min}, respectively, at the core top are 29.4 °C and 26.8 °C, which are in very close agreement with modern day SST observations. Mean SST varies little during the past 80,000 cal yr. The temperature of the warmest month (T_{max}) fluctuates between 28.3 °C and 29.8 °C, and the temperature of the coolest month (T_{min}) fluctuates between 26.1 °C and 28.2 °C. There is a low correlation between T_{max} and T_{min} of r^2=0.37.

The lack of temperature change is consistent with the relatively high abundance of the mixed-layer dweller *G. ruber* (white), an indicator of warm SST. The highest SST is recorded at 8000 ^{14}C cal yr BP when the mixed-layer dwellers (particularly *G. quadrilobatus*) are most abundant (see Figs. 5 and 6).

Temperature estimates for the LGM and Isotope Stage 4 are within errors of the core top values, although these periods correspond to the lowest abundances of the mixed-layer dwellers. Any SST change here is close to the error of the technique, and is therefore difficult to resolve. Seasonality varied between 1.5 and 3.0 °C, and is lowest during the periods of high SST during the Holocene. Seasonality increased during the relatively cooler intervals (see Fig. 6).

6. Discussion

6.1. The deep chlorophyll maximum layer

Changes in the relative abundances of planktonic foraminifera within core SHI 9016, which inhabits different water depth levels, indicate that the vertical structure of the water column changed through time

(Figs. 5 and 6). The species *N. dutertrei* and *N. pachyderma* are more abundant from approximately 48,000 to 15,000 cal yr BP, indicating a more nutrient-rich, intermediate photic zone than present. These conditions are usually associated with an enhancement of the DCM. The appearance of the temperate species *N. pachyderma* at the latitude of core SHI 9016 can only be accounted for by the presence of cool, nutrient-rich waters at depth.

There is a regional pattern of DCM development in the Indonesian Archipelago during MIS 3 and 2. In the northern Molucca Sea, Barmawidjaja et al. (1993) found higher relative abundances of *N. dutertrei* and *N. pachyderma* during the past ~27,000 yr. Barmawidjaja et al.'s (1993) explanation of these results was that the upper part of the thermocline was residing consistently above the light compensation depth (i.e., an enhancement of the DCM). This implies that the glacial temperatures, at the base of the euphotic layer, were lower than today (Barmawidjaja et al., 1993). Similarly, Linsley et al. (1985) and Ding et al. (2002) found that *N. dutertrei* and *N. pachyderma* were approximately 20% and 10% more abundant, respectively, in the Sulu Basin during MIS 3 and 2. Ding et al. (2002) also found that *N. pachyderma* increased to 10–20% during the LGM in cores from the Makassar Strait and northeastern Indian Ocean.

The persistence of *G. ruber* throughout the core indicates the continual presence of a tropical mixed layer. In addition, *G. menardii* and *P. obliquiloculata* are not abundant during MIS 3 and indicate that upwelling did not occur. However, the increased abundance of thermocline dwellers in the assemblages during MIS 2 and 3 indicates that the mixed layer was thinner during this time. At ~15,000 cal yr BP, an increase in the relative abundance of oligotrophic species, especially *G. quadrilobatus*, indicates that the mixed layer thickens while the DCM layer declines through to the Holocene (Fig. 5). This event was very similar to the timing of DCM removal in core K12 in the Molucca Sea at 14,000 yr BP (Barmawidjaja et al., 1993).

6.2. The Northwest Monsoon '*switch*'

In the modern Banda Sea, as noted above, the mixed layer thins seasonally during the SE Monsoon and is thickest during the NW Monsoon. The observation that the mixed layer was significantly thinner in the Banda Sea during MIS 3 and 2, until ~15,000 cal yr BP, points to a reduction in the influence of the NW Monsoon. This result closely matches the estimate of NW Monsoon 'switching on' in Australia at 14,000 yr BP estimated by Wyrwoll and Miller (2001) and van der Kaars and De Deckker (2002).

We suggest that the ITCZ was north of the Banda Sea during MIS 3 and 2 most, if not all, of the year, promoting the trade winds to blow across the Banda Sea, without incursions of the ITCZ into northern Australia. This essentially has the effect of the operation of a 'perpetual' SE Monsoon (c.f. Barrows and Juggins, 2005). Stott et al. (2004) have suggested that even in the early Holocene, the ITCZ was further north than present in the western tropical Pacific Ocean. In core SHI 9016, we see that the NW Monsoon strengthens in the early Holocene. However, at ~7500 yr BP, a small spike in T_{mean} can be seen and a positive response in thermocline species suggests a momentary strengthening of the SE Monsoon.

Studies of the vegetation history of areas flanking the western Indonesian Throughflow (Barmawidjaja et al., 1993; van der Kaars and Dam, 1995) indicate that MIS 3 was drier and this is attributed to the reduction of the NW Monsoon. The vegetation history of the Indonesian region indicates drier climates culminating at the LGM (van der Kaars, 1989; Barmawidjaja et al., 1993; van der Kaars and Dam, 1995; Wang et al., 1999; van der Kaars et al., 2000). Clay analysis by Gingele et al. (2001) also indicates a dry climate during the LGM. In addition, the vegetation history reveals an increase in wetter climatic conditions from 17 to 14 ka (van der Kaars, 1989; Barmawidjaja et al., 1993; Wyrwoll and Miller, 2001). Northern Australia studies by Magee et al. (1995), Magee and Miller (1998), Croke et al. (1999), Veeh et al. (2000), English et al. (2001), van der Kaars and De Deckker (2002), Hesse and McTainsh (2003), and Hesse et al. (2004) also indicate drier conditions during MIS 3 and 2 and suggest greater influence of the SE Monsoon.

The NW Monsoon seems to strengthen at 10,300 cal yr BP, indicating that the biannual monsoonal system was most intense at this time (Fig. 6). Similarly, seasonality is high at 65,000–70,000 cal yr BP, and at 78,000 cal yr BP. Magee et al. (1995) suggested that the NW Monsoon promoted wetter phases in the

Lake Eyre catchment of central Australia at 125,000 yr BP, 80,000 yr BP, 65,000 yr BP, and 40,000 yr BP. Although our record does not extend back to 125,000 cal yr BP, we see similar timings for the incursion of the NW Monsoon across the Banda Sea at 80,000 and 65,000 yr BP. In contrast, Gingele et al. (2002) suggested that the NW Monsoon was more dominant during 70,000–55,000 and 35,000–20,000 yr BP in the eastern Indian Ocean, due to the direction and source of clays in the South Java Current.

6.3. Sea-surface temperature and regional aridity during the LGM

Our SST estimates do not indicate a significant change in SST during the LGM in core SHI 9016 and that most of the change in fauna is due to changes in mixed-layer depth as a response to surface wind forcing. The main change in temperature is at 150 m water depth which suggests the movement of the thermocline into the photic zone during MIS 3 and 2 (Fig. 6).

Surface temperature estimates around the Indonesian Archipelago vary widely and are often contradictory. However, these estimates are over a wide geographical area and from different oceanographic settings. The lack of evidence for cooling during the LGM supports the findings of Ahmad et al. (1995) and Linsley (1996), but differs from the SST estimates of Thunell et al. (1994) and Ding et al., 2002, and also Mg/Ca results of Lea et al. (2000), Stott et al. (2002), Visser et al. (2003), and Stott et al. (2004). Ding et al. (2002) found a reduction in SST of 1 °C in the Makassar Strait and a reduction of 1.9 °C in the northeastern Indian Ocean. Stott et al. (2002) also found a 2 °C reduction during the LGM, using Mg/Ca analyses, at the eastern edge of the Indonesian Archipelago. Furthermore, recent studies by Thunell et al. (1994) estimate 0–1.5 °C cooling, whereas Lea et al. (2000) and Visser et al. (2003) estimate 3 °C cooling during the LGM in the western equatorial Pacific and the Makassar Strait, respectively. We note that the SST reduction of 1 °C in the Makassar Strait in the study by Ding et al. (2002) used the AUSMAT-F3 database (Barrows et al., 2000), but in this study of core SHI 9016, we use an updated version (AUSMAT-F4). Thunell et al. (1994) also used the older database of Prell (1985) with the MAT. Taken together, these studies indicate that the Throughflow was not cooler than present by more than ~3 °C.

Without significant SST change, the $\delta^{18}O$ difference between the LGM and present ($\Delta\delta^{18}O$) of 0.4‰ in SHI 9016 can be explained by sea-surface salinity increase due to decreased precipitation during the LGM. De Deckker et al. (2003) believe that the altered configurations of the land margins during the LGM may have increased the salinity of surface water. Ganssen et al. (1989) found that the $\Delta\delta^{18}O$ was 1.2‰ in the Banda Sea. This is close to the estimated value of the ice volume effect of 1.0–1.1‰ of Schrag et al. (1996). However, Ahmad et al. (1995) found a $\Delta\delta^{18}O$ of 1.6 ‰ in core SHI 9014 also in the Banda Sea (Fig. 1). They supported CLIMAP's estimate of no SST change during the LGM and explained the $\Delta\delta^{18}O$ of 0.4‰ as a result of increased salinity. A $\Delta\delta^{18}O$ of 0.8‰ was reported by Barmawidjaja et al. (1993) for the northern Molucca Sea in core K12 (Fig. 1). This indicates that during the LGM, the northern Molucca Sea surface water was either 3 °C cooler or was 1.5–1.9‰ saltier, or some combination of the two parameters (Barmawidjaja et al., 1993). Martinez et al. (2002) showed that there was a ~3 °C SST change within core K12, based on planktonic foraminiferal assemblages, favouring the former interpretation. However, evidence from the semi-isolated Sulu Sea basin by Oppo et al. (2003) suggests that salinity did not change and Visser et al. (2003) suggests that an increase in salinity was not apparent in the Makassar Strait and decreased temperature explained all of the $\delta^{18}O$ residuals.

On a regional scale, salinity appears to be higher during the Pleistocene; Ahmad et al. (1995) and Linsley (1996) found that salinity was more influential than SST during the LGM. This is confirmed by the study of Martinez et al. (1997) and De Deckker et al. (2003), which examined $\delta^{18}O$ residuals for the entire WP region. Presently, during the SE Monsoon, sea-surface salinities are greater than during the NW Monsoon 'wet season' by ~3‰ (Wyrtki, 1961). Again, there seems to be evidence that the SE Monsoon was the dominant phase of the Australasian Monsoon during MIS 3 and 2 due to the apparent reduction of precipitation.

Regional vegetation changes (Wang et al., 1999; van der Kaars and Dam, 1995; van der Kaars et al.,

2000, 2001; Haberle et al., 2001; Hope, 2001) indicate that precipitation was reduced during the LGM and this might largely explain the increase in salinity. Modified clay mineralogies, potentially related to changes in river discharge, appear to support reduced precipitation during the LGM (Gingele et al., 2001).

6.4. The Indonesian Throughflow

Studies conducted in the eastern Indian Ocean indicate a stronger Java upwelling system between the LGM and today (Martinez et al., 1998, 1999; Takahashi and Okada, 2000; Gingele et al., 2001). In addition, palaeoproductivity proxy investigations by Müller and Opdyke (2000) in the Timor passage indicate increased nutrients in the mixed layer during MIS 2. Müller and Opdyke (2000) concluded that during the LGM, there was higher surface ocean productivity than during the Holocene due to a reduction or absence of the low-salinity cap.

Presently, upwelling along the coast of Java operates between August and September (Wyrtki, 1962) due to the SE Monsoon. However, blooms associated with increased nutrients are limited due to the capping effect of the low-salinity boundary layer (sensu Lukas and Lindstrom, 1991) of the Throughflow, which increases during the SE Monsoon (Tomczak and Godfrey, 1994). A more dynamic and productive Java upwelling system encouraged by the SE Monsoon is indicated in studies by Martinez et al. (1999) and Gingele et al. (2002). With less precipitation in the area during the LGM, it is possible that characteristics of the present-day, low-salinity boundary layer were not applicable.

7. Conclusion

We establish that the NW Monsoon over northern Australian and the Banda Sea was not operating during the LGM and 'switched on' about 14,000 yr ago. Therefore, there were no excursions of the ITCZ south of the Banda Sea that today bring moisture to Australia. A scenario where the NW Monsoon does not operate would create a situation analogous to the SE Monsoon operating throughout the year because the trade winds would blow continually across the Banda Sea. Like today, this would promote a thinner mixed layer and a shallower thermocline. This situation is supported by the planktonic foraminifera data, which indicate that the mixed layer was thinner during the LGM and thickened at the beginning of the Holocene.

Acknowledgements

We thank Dr. F. Guichard (CEA/CNRS, Gif-sur-Yvette, France) for making core SHI 9016 available for this study. Dr. George Chaponière helped with taxonomic aspects of the planktonic foraminifers and Joe Cali carried out the isotopic analyses, which were funded through an ARC grant, as well as an ANU grant, awarded to Patrick De Deckker.

References

Ahmad, S.M., Guichard, F., Hardjawidjaksana, K., Adisaputra, M.K., Labeyrie, L.D., 1995. Late Quaternary paleoceanography of the Banda Sea. Marine Geology 122, 385–397.

Barmawidjaja, B.M., Rohling, E.J., van der Kaars, W.A., Vergnaud Grazzini, C., Zachariasse, W.J., 1993. Glacial conditions of the northern Molucca Sea region (Indonesia). Palaeogeography, Palaeoclimatology, Palaeoecology 101, 147–167.

Barrows, T.T., Juggins, S., 2005. Sea-surface temperatures around the Australian margin and Indian ocean during the Last Glacial Maximum. Quaternary Science Reviews 24 (7–9), 1017–1047.

Barrows, T.T., Juggins, S., De Deckker, P., Thiede, J., Martinez, J.I., 2000. Sea-surface temperatures of the southwest Pacific Ocean during the last glacial maximum. Paleoceanography 15 (1), 95–109.

Bé, A.W.H., Hutson, W.H., 1977. Ecology of planktonic foraminifera and biogeographic patterns of life and fossil assemblages in the Indian Ocean. Micropaleontology 23 (4), 369–414.

Bowman, G.M., 1985. Oceanic reservoir correction for marine radiocarbon dates from northwestern Australia. Australian Archaeology 20, 58–67.

Bray, N.A., Hautala, S., Chong, J., Pariwono, J., 1996. Large-scale sea level, thermocline, and wind variations in the Indonesian Throughflow region. Journal of Geophysical Research 101, 12239–12254.

Chapronière, G.C.H., 1991. Pleistocene to Holocene planktic foraminiferal biostratigraphy of the Coral Sea, offshore Queensland, Australia. BMR Journal of Australian Geology and Geophysics 12 (3), 195–221.

Croke, J.C., Magee, J.W., Wallensky, E.P., 1999. The role of the Australian Monsoon in the western catchment of Lake Eyre, central Australia, during the Last Interglacial. Quaternary International 57/58, 71–80.

De Deckker, P., Tapper, N.J., van der Kaars, S., 2003. The status of the Indo-Pacific Warm Pool and adjacent land at the last glacial maximum. Global and Planetary Change 35 (1–2), 25–35.

Ding, X., Guichard, F., Bassinot, F., Labeyrie, L., Fang, N.Q., 2002. Evolution of heat transport pathways in the Indonesian Archipelago during last deglaciation. Chinese Science Bulletin 47 (22), 1912–1917.

English, P., Spooner, N.A., Chappell, J., Questiaux, D.G., Hill, N.G., 2001. Lake Lewis basin, central Australia: environmental evolution and OSL chronology. Quaternary International 83–85, 81–102.

Fairbanks, G.R., Wiebe, P.H., 1980. Foraminifera and chlorophyll maximum: vertical distribution, seasonal succession, and paleoceanographic significance. Science 209, 1524–1525.

Ganssen, G., Troelstra, S.R., Faber, B., van der Kaars, W.A., Situmorang, M., 1989. Late Quaternary palaeoceanography of the Banda Sea, Eastern Indonesian piston cores (Snellius-II Expedition, cruise G5). Netherlands Journal of Sea Research 24 (4), 491–494.

Gieskes, W.W.C., Kraay, G.W., Nontji, A., Setiapermana, D., Sutomo, 1988. Monsoonal alteration of a mixed and layered structure in the phytoplankton of the euphotic zone of the Banda Sea (Indonesia): a mathematical analysis of algal pigment fingerprints. Netherlands Journal of Sea Research 22 (2), 123–137.

Gingele, F.X., De Deckker, P., Hillenbrand, C.D., 2001. Late Quaternary fluctuations of the Leeuwin Current and palaeoclimates on the adjacent landmasses: clay minerals evidence. Australian Journal of Earth Sciences 48, 867–874.

Gingele, F.X., De Deckker, P., Girault, A., Guichard, F., 2002. History of the South Java Current over the past 80 ka. Palaeogeography, Palaeoclimatology, Palaeoecology 183 (3–4), 247–260.

Godfrey, J.S., 1996. The effect of the Indonesian Throughflow on ocean circulation and heat exchange with the atmosphere: a review. Journal of Geophysical Research 101, 12217–12237.

Gordon, A.L., 1986. Interocean exchange of thermocline water. Journal of Geophysical Research 91, 5037–5046.

Haberle, S.G., Geoff, S., Hope, G.S., van der Kaars, S., 2001. Biomass burning in Indonesia and Papua New Guinea: natural and human induced fire events in the fossil record. Palaeogeography, Palaeoclimatology, Palaeoecology 171 (3–4), 25–268.

Hautala, S.L., Reid, J.L., Bray, N., 1996. The distribution and mixing of Pacific water masses in the Indonesian Seas. Journal of Geophysical Research 101, 12375–12389.

Hayward, T.L., 1987. The nutrient distribution and primary production in the central North Pacific. Deep-Sea Research 34, 1593–1627.

Hemleben, C., Spindler, M., Anderson, O.R., 1989. Modern Planktonic Foraminifera. Springer-Verlag, New York.

Hesse, P.P., McTainsh, G.H., 2003. Australian dust deposits: modern processes and the Quaternary record. Quaternary Science Reviews 22, 2007–2035.

Hesse, P.P., Magee, J.W., van der Kaars, S., 2004. Late Quaternary climates of the Australian arid zone. Quaternary International 118–119, 87–102.

Hilbrecht, H., 1996. Extant planktic foraminifera and the physical environment in the Atlantic and Indian Oceans. Mitteilungen aus dem Geologischen Institut der Eidgen. Technischen Hochschule und der Universität Zürich, Neue Folge 300, 1–93.

Hobbs, J.E., 1998. In: Hobbs, J.E., Lindesay, J.A., Bridgman, H.A. (Eds.), Climates of the Southern Continents: Present, Past and Future. John Wiley and Sons Publishers, West Sussex, England, pp. 63–100.

Hope, G., 2001. Environmental change in the Late Pleistocene and later Holocene at Wanda site, Soroako, South Sulawesi, Indonesia. Palaeogeography, Palaeoclimatology, Palaeoecology 171 (3–4), 129–145.

Kinkade, C., Marra, J., Langdon, C., Knudson, C., Ilahude, A.G., 1997. Monsoonal differences in phytoplankton biomass and production in the Indonesian Sea: tracing vertical mixing using temperature. Deep-Sea Research I 44 (4), 581–592.

Lea, D.W., Pak, D.K., Spero, H.J., 2000. Climate impact of the late Quaternary equatorial Pacific sea surface temperature variations. Science 289, 1719–1724.

Levitus, S., Boyer, T.P., 1994. World Ocean Atlas (WOA), Temperature, volume 4. NOAA Atlas and CD, U.S. Department of Commerce, Washington, DC. National Oceanographic Data Center, Silver Spring, Maryland.

Levitus, S., Burgett, R., Boyer, T.P., 1994. World Ocean Atlas (WOA), Salinity, volume 3. NOAA Atlas and CD, U.S. Department of Commerce, Washington, DC. National Oceanographic Data Center, Silver Spring, Maryland.

Linsley, B., 1996. Oxygen-isotope record of sea level and climate variations in the Sulu Sea over the past 150,000 years. Nature 380, 234–237.

Linsley, B.K., Thunell, R.C., Morgan, C., Williams, D.F., 1985. Oxygen minimum expansion in the Sulu Sea, western equatorial Pacific, during the last glacial low stand of sea level. Marine Micropaleontology 9, 395–418.

Lukas, R., Lindstrom, E.J., 1991. The mixed layer of the western equatorial Pacific Ocean. Journal of Geophysical Research 96, 3343–3357.

Magee, J.W., Miller, G.H., 1998. Lake Eyre palaeohydrology from 60 ka to the present: beach ridges and glacial maximum aridity. Palaeogeography, Palaeoclimatology, Palaeoecology 144, 307–329.

Magee, J.W., Bowler, J.M., Miller, G.H., Williams, D.L.G., 1995. Stratigraphy, sedimentology, chronology and palaeohydrology of Quaternary lacustrine deposits at Madigan Gulf, Lake Eyre, South Australia. Palaeogeography, Palaeoclimatology, Palaeoecology 113, 3–42.

Martinez, J.I., De Deckker, P., Chivas, A.R., 1997. New estimates for salinity changes in the Western Pacific Warm Pool during the last glacial maximum: oxygen-isotope evidence. Marine Micropaleontology 32, 311–340.

Martinez, J.I., Taylor, L., De Deckker, P., Barrows, T., 1998. Planktonic foraminifera from the eastern Indian Ocean: distribution and ecology in relation to the Western Pacific Warm Pool (WPWP). Marine Micropaleontology 34, 121–151.

Martinez, J.I., De Deckker, P., Barrows, T., 1999. Palaeoceanography of the last glacial maximum in the eastern Indian Ocean:

planktonic foraminifera evidence. Palaeogeography, Palaeoclimatology, Palaeoecology 147, 73–99.

Martinez, J.I., De Deckker, P., Barrows, T.T., 2002. Palaeoceanography of the western Pacific warm pool during the last glacial maximum: long-term climatic monitoring of the maritime continent. Bridging Wallaces Line: The Environmental and Cultural History and Dynamics of the SE-Asian–Australian Region. Advances in Geoecology 34, 147–172.

Martinson, D.G., Pisias, N.G., Hays, J., Imbrie, J., Theodore, C.M., Moore, J.R., Shackleton, N.J., 1987. Age resolution and the orbital theory of the ice ages: development of a high resolution 0–300,000-year chronostratigraphy. Quaternary Research 27, 1–22.

Molcard, R., Fieux, M., Ilahude, A.G., 1996. The Indo-Pacific Throughflow in the Timor passage. Journal of Geophysical Research 101, 12411–12420.

Müller, A., Opdyke, B.N., 2000. Glacial–interglacial changes in nutrient utilization and palaeoproductivity in the Indonesian Throughflow sensitive Timor Trough, easternmost Indian Ocean. Paleoceanography 15, 85–94.

Oppo, D.W., Linsley, B.K., Rosenthal, Y., Dannenmann, S., Beaufort, L., 2003. Orbital and suborbital climate variability in the Sulu Sea, western tropical Pacific. Geochemistry Geophysics and Geosystems 4 (1), 1–20.

Prell, W.L., 1985. The stability of low-latitude sea-surface temperatures: an evaluation of the CLIMAP reconstruction with emphasis on the positive SST anomalies. Spec. Pub. TRO25. Department of Energy, Washington, D.C.

Saito, T., Thompson, P.R., Berger, D., 1981. Systematic Index of Recent and Pleistocene Planktonic Foraminifera. University Press, Tokyo.

Singh, G., Agrawal, D.P., 1976. Radiocarbon evidence for deglaciation in north-western Himalaya, India. Nature 260, 232.

Schrag, D.P., Hampt, G., Murray, D.W., 1996. Pore fluid constraints on the temperature and oxygen isotopic composition of the glacial ocean. Science 272, 1930–1932.

Southon, J., Kashgarian, M., Fontugne, M., Metivier, B., Yim, W.W.-S., 2002. Marine reservoir corrections for the Indian Ocean and Southeast Asia. Radiocarbon 44, 167–180.

Stott, L., Poulsen, C., Lund, S., Thunell, R., 2002. Super ENSO and global climate oscillations at millennial time scales. Science 297, 222–226.

Stott, L., Cannariato, K., Thunell, R., Haug, G.H., Athanasios, K., Lund, S., 2004. Decline of surface temperature and salinity in the western tropical Pacific Ocean in the Holocene epoch. Nature 431, 56–59.

Stuiver, M., Reimer, P.J., Bard, E., Beck, W.E., Burr, G.S., Hughen, K.A., Kromer, B., McCormac, F.G.V.D., Plicht, J., Spurk, M., 1998. INTCAL98 radiocarbon age calibration 0–24,000 BP. Radiocarbon 40, 1041–1083.

Takahashi, K., Okada, H., 2000. The paleoceanography for the last 30,000 years in the Southeastern Indian Ocean by means of calcareous nannofossils. Marine Micropaleontology 40, 83–103.

Thompson, P.R., Bé, A.W.H., Duplessy, J.C., Shackleton, N.J., 1979. Disappearance of pink-pigmented *Globigerinoides ruber* at 125,000 yr BP in the Indian and Pacific Oceans. Nature 280 (5723), 554–558.

Thunell, R., Anderson, D., Gellar, D., Miao, Q., 1994. Sea-surface temperature estimates for the Tropical Western Pacific during the Last Glaciation and their implications for the Pacific Warm Pool. Quaternary Research 41, 255–264.

Tisnérat-Laborde, N., Poupeau, J.J., Tannau, J.F., Paterne, M., 2001. Development of a semi-automated system for routine preparation of carbonate samples. Radiocarbon 43, 299–304.

Tomczak, M., Godfrey, J.S., 1994. Regional Oceanography: An Introduction. Pergamon Press, Oxford.

Troelstra, S.R., Kroon, D., 1989. Note on extant planktonic foraminifera from the Banda Sea, Indonesia (Snellius-II Expedition, cruise G5). Netherlands Journal of Sea Research 24 (4), 459–463.

Troelstra, S.R., Klaver, G.J., Kleijne, A., Kroon, D., Van Marle, L.J., Meyboom, W., van de Paverd, P.J., Situmorang, M., van Waveren, I.M., 1989. Actuomicropalaeontology and sediment distribution of three transects across the Banda Arc, Indonesia (Snellius-II Expedition, Cruise G5). Netherlands Journal of Sea Research 24 (4), 477–489.

van der Kaars, W.A., 1989. Aspects of late Quaternary palynology of eastern Indonesian deep-sea cores. Netherlands Journal of Sea Research 24 (4), 495–500.

van der Kaars, W.A., Dam, M.A.C., 1995. A 135,000-year old record of vegetational and climatic change from the Bandung area, West-Java, Indonesia. Palaeogeography, Palaeoclimatology, Palaeoecology 117 (1–2), 55–71.

van der Kaars, S., De Deckker, P., 2002. A Late Quaternary pollen record from deep-sea core FR10/95, GC17 offshore Cape Range Peninsula, northwestern Western Australia. Review of Palaeobotany and Palynology 120 (1–2), 17–39.

van der Kaars, S., Wang, X., Kershaw, P., Guichard, F., Setiabudi, D.A., 2000. A late Quaternary palaeoecological record from the Banda Sea, Indonesia: patterns of vegetation, climate and biomass burning in Indonesia and northern Australia. Palaeogeography, Palaeoclimatology, Palaeoecology 155, 135–153.

van der Kaars, S., Penny, D., Tibby, J., Fluin, J., Dam, R.A.C., Suparan, P., 2001. Late Quaternary palaeoecology, palynology and palaeolimnology of a tropical lowland swamp: Rawa Danau, West-Java, Indonesia. Palaeogeography, Palaeoclimatology, Palaeoecology 171 (3–4), 185–212.

van Iperen, J.M., van Bennekom, A.J., van Weering, T.C.E., 1993. Diatoms in surface sediments of the Indonesian Archipelago and their relation to hydrography. Hydrobiologia 269/270, 113–128.

Veeh, H.H., McCorkle, D.C., Heggie, D.T., 2000. Glacial/interglacial variations of sedimentation on the West Australian continental margin: constraints from excess ^{230}Th. Marine Geology 166, 11–30.

Visser, K., Thunell, R., Stott, L., 2003. Magnitude and timing of temperature change in the Indo-Pacific warm pool during glaciation. Nature 421, 152–155.

Waliser, D.E., Graham, N.E., 1993. Convective cloud system and Warm-Pool sea surface temperatures: coupled interactions and self regulation. Journal of Geophysical Research 98, 12881–12893.

Wang, X., van der Kaars, W.A., Kershaw, P., Bird, M., Jansen, F., 1999. A record of fire, vegetation and climate through the last three glacial cycles from the Lombok Ridge core G6-4, eastern Indian Ocean, Indonesia. Palaeogeography, Palaeoclimatology, Palaeoecology 147, 241–256.

Wijffels, S.E., Bray, N., Hautala, S., Meyers, G., Morawitz, W.M.L., 1996. The WOCE Indonesian Throughflow repeat hydrology sections: 110 and IR6. International WOCE Newsletter 24, 25–28.

Wyrtki, K., 1961. Physical oceanography of Southeast Asian waters, Scientific results of maritime investigations of the South China Sea and Gulf of Thailand 1959–1961, NAGA Rep. 2, Scripps Institute of Oceanography, La Jolla, California.

Wyrtki, K., 1962. The upwelling in the region between Java and Australia during the south-east monsoon. Australian Journal of Marine and Freshwater Research 13 (3), 217–225.

Wyrtki, K., 1987. Indonesian Throughflow and the associated pressure gradient. Journal of Geophysical Research 92, 12941–12946.

Wyrwoll, K.H., Miller, G.H., 2001. Initiation of the Australian summer monsoon 14,000 years ago. Quaternary International 83–85, 119–128.

Yan, X.H., Ho, C.R., Zheng, Q., Klemas, V., 1992. Temperature and size variabilities of the Western Pacific Warm Pool. Science 258, 1643–1645.